Accurate experimental characterization of the labile N–Cl bond in N-chloro-N'-(*p*-fluorophenyl)-benzamidine crystal at 17.5 K

Riccardo Destro,[1] Mario Barzaghi,[2] Raffaella Soave,[3] Pietro Roversi[4,5] and Leonardo Lo Presti[1,6,*]

1 Università degli Studi di Milano, Department of Chemistry, Via Golgi 19, 20133 Milano (Italy)

2 Consiglio Nazionale delle Ricerche (CNR), Piazzale Aldo Moro 7, 00185 Roma (Italy)

3 Consiglio Nazionale delle Ricerche (CNR), Istituto di Scienze E Tecnologie Chimiche "Giulio Natta" (SCITEC), Via Golgi 19, 20133 Milano (Italy)

4 Consiglio Nazionale delle Ricerche - IBBA, Via Bassini 15, 20133 Milano (Italy)

5 Leicester Institute of Chemical and Structural Biology and Department of Molecular and Cell Biology, University of Leicester, Henry Wellcome Building, Lancaster Road, Leicester LE1 7HR, United Kingdom

6 Istituto Nazionale di Fisica Nucleare (INFN), Laboratori Nazionali di Frascati, Frascati (Italy)

* To whom correspondence should be addressed: leonardo.lopresti@unimi.it

SUPPLEMENTARY MATERIAL

S1. Details of the data collection

S1.1 First sample

Unaware of the relatively high vapor pressure of this compound, we glued a sample (ground to an approximate sphere 0.5 mm in diameter) on the tip of a glass fiber at the center of the vacuum shroud ($P \approx 10^{-8}$ mbar) without enclosing the crystal into a protective medium, and the temperature was gradually lowered. In the few hours necessary to reach the lowest temperature the crystal diameter decreased to 0.45 mm, then the volume remained unchanged for the following ~340 hours of exposure to X-rays at constant low pressure and low T. But visual inspection and profile analysis showed that a crystal fracture had occurred during data collection, and the 12158 intensities measured from this sample were discarded.

S1.2 Second sample

The first stop, that lasted 86 days, occurred after 336.7 hours of exposure of the crystal to X-rays, with the generator operating at high power (50kV and 25mA) for 299.7 h, and at low power (30kV and 3mA) for the following 37 h. The lower current radiation was employed to re-measure low-angle data, to minimize possible problems associated with nonlinearity of the photon counting system. When the crystal was removed from the cryostat and brought back to room temperature, its enclosure into the capillary showed very effective, since no reduction of volume nor fractures were noticeable, but it was no longer transparent and appeared pale yellow. This first portion of the data set comprised 13526 diffracted intensities.

Before restarting the regular data collection the crystal was exposed to the high-power X-rays for 72.3 hours, to perform background and profile measurements necessary for the subsequent treatment of truncation errors, according to the procedure regularly applied in our laboratory for accurate charge-density studies.[1–6] A second stop, lasting four days, was required by a sudden failure of the vacuum system just after the resumption of intensity measurements, with only 603 new data collected. At the opening of the cryostat the crystal color showed to be slightly darker then at the beginning of this data-collection step. After replacement of some cryostat components, a low temperature around 17 K was reached and maintained until the end of the data collection, more than 300 hours later, when the crystal color had become brown.

S2. List of Cambridge Structural Database reference codes employed to study the N–Cl bond

AZCFOM01
ENAJIO
FEVNUP
GUGREH
NUJJAF
NUXXOV
PASJAV
RAQBIX
SEMHOI
TIYDAI
TIYDOW
TIYDOW01
TIYFAK
TUWDIY
XOLYAA

S3. Input stream for periodic quantum simulations (CRYSTAL)

```
N-CL 20 K exp geom P3(1)
CRYSTAL
0 0 0
144
10.0227 9.8795 120.0
27
17   0.089013  0.118406  0.000000
9   -0.160927 -0.794176  0.140331
7    0.209995  0.098324  0.115595
7    0.053783 -0.170978  0.078869
6    0.172367 -0.044991  0.136584
6    0.272930 -0.061649  0.238114
6    0.210421 -0.143198  0.358411
6    0.308218 -0.149467  0.455553
6    0.467106 -0.074594  0.432856
6    0.528832  0.004856  0.312118
6    0.431602  0.011242  0.214466
6    0.005815 -0.328214  0.103924
6    0.108419 -0.384318  0.110701
6    0.051902 -0.542012  0.127067
6   -0.106276 -0.640499  0.132155
6   -0.210227 -0.587647  0.127455
6   -0.152639 -0.429736  0.114630
1    0.087910 -0.195190  0.375840
1    0.261490 -0.204300  0.553500
1    0.542960 -0.078300  0.509220
1    0.651200  0.060410  0.294370
1    0.479520  0.074300  0.121750
1    0.230980 -0.308120  0.102840
1    0.126800 -0.590660  0.131650
1   -0.333690 -0.661900  0.133580
1   -0.228850 -0.384140  0.110880
1   -0.016150 -0.155980  0.014100
ATOMORDE
SYMMOPS
OPTGEOM
ATOMONLY
MAXCYCLE
100
ENDOPT
ENDGEOM
17 10
0 0 7 2.0 1.0
  69507.990945      0.00054314897497
  10426.156880      0.00419904639610
  2373.2334061      0.02159214167900
  671.56420071      0.08459885009400
  218.41999790      0.24757249724000
  77.572249714      0.47016930228000
  28.888815277      0.37436370716000
0 0 3 2.0 1.0
  127.10527185      0.02518216660300
  39.339582961      0.10786112456000
  7.6740679989     -0.27408821574000
0 0 2 2.0 1.0
  3.8745627630      1.32138750140000
  1.8385832573      0.68636955368000
0 0 1 0.0 1.0
  0.4498594500      1.00000000000000
0 0 1 0.0 1.0
  0.1363703100      1.00000000000000
0 2 5 6.0 1.0
  666.50423284      0.00236326638360
  157.64241690      0.01887930037400
  50.262520978      0.08720634127300
  18.536078105      0.25285612970000
  7.2940532777      0.43507154820000
0 2 1 5.0 1.0
  2.80149164000     1.00000000000000
0 2 1 0.0 1.0
  0.78964278000     1.00000000000000
0 2 1 0.0 1.0
  0.21056105000     1.00000000000000
0 3 1 0.0 1.0
  0.23728440000     1.00000000000000
9 8
0 0 6 2.0 1.0
  35479.100441      0.00021545014888
  5318.4728983      0.00167006865270
  1210.4810975      0.00867332114760
  342.85518140      0.03504993317500
  112.01943181      0.11165320133000
  40.714740248      0.25988506647000
0 0 2 2.0 1.0
  16.039678111      0.39422966880000
  6.5038186740      0.24998238551000
0 0 1 0.0 1.0
  1.4420074900      1.00000000000000
0 0 1 0.0 1.0
  0.4597725800      1.00000000000000
0 2 4 5.0 1.0
  80.233900483      0.00636859991340
  18.594010743      0.04430314353000
  5.6867902653      0.16867248708000
  1.9511006294      0.36166346255000
0 2 1 0.0 1.0
  0.6922845200      1.00000000000000
0 2 1 0.0 1.0
  0.1983553200      1.00000000000000
0 3 1 0.0 1.0
  1.0631263500      1.00000000000000
7 8
0 0 6 2.0 1.0
  19730.800647      0.00021887984991
  2957.8958745      0.00169607088030
  673.22133595      0.00879546035380
  190.68249494      0.03535938260500
  62.295441898      0.11095789217000
  22.654161182      0.24982972552000
0 0 2 2.0 1.0
  8.9791477428      0.4062389614800
  3.6863002370      0.2433821717600
0 0 1 0.0 1.0
  0.7865398200      1.0000000000000
0 0 1 0.0 1.0
  0.2677997200      1.0000000000000
0 2 4 3.0 1.0
  49.200380510      0.0055552416751
  11.346790537      0.0380523797230
  3.4273972411      0.1495367102900
  1.1785525134      0.3494930523000
0 2 1 0.0 1.0
  0.3780331700      1.0000000000000
0 2 1 0.0 1.0
  0.1473661500      1.0000000000000
0 3 1 0.0 1.0
  0.3612294900      1.0000000000000
6 8
0 0 6 2.0 1.0
  13575.349682      0.00022245814352
  2035.2333680      0.00172327382520
  463.22562359      0.00892557153140
  131.20019598      0.03572798450200
  42.853015891      0.11076259931000
  15.584185766      0.24295627626000
0 0 2 2.0 1.0
  6.2067138508      0.41440263448000
  2.5764896527      0.23744968655000
0 0 1 0.0 1.0
  0.4941102000      1.00000000000000
0 0 1 0.0 1.0
  0.1644071000      1.00000000000000
0 2 4 2.0 1.0
  34.697232244      0.00533336578050
  7.9582622826      0.03586410909200
  2.3780826883      0.14215873329000
  0.8143320818      0.34270471845000
0 2 1 0.0 1.0
  0.5662417100      1.00000000000000
0 2 1 0.0 1.0
```

```
  0.1973545000      1.00000000000000
0 3 1 0.0 1.0
  0.5791584200      1.00000000000000
1 4
0 0 3 1.0 1.0
  34.061341000      0.00602519780
  5.1235746000      0.04502109400
  1.1646626000      0.20189726000
0 0 1 0.0 1.0
  0.5157455100      1.00000000000
0 0 1 0.0 1.0
  0.1795111000      1.00000000000
0 2 1 0.0 1.0
  0.5000000000      1.00000000000
99 0
ENDBASIS
DFT
PBE0
ENDDFT
SHRINK
4 4
GRIMME
1.05 20. 25.
5
1  0.14 1.001
6  1.75 1.452
7  1.23 1.397
9  0.75 1.287
17 5.07 1.639
LEVSHIFT
5 0
FMIXING
30
TOLINTEG
8 8 8 8 16
PPAN
ENDSCF
STOP
```

S4. Estimation of the absorbed dose

The operational parameters of the current data collections are $\lambda = 0.71073$ Å at a nominal 50 kV x 25 mA (1250 W) power of the generator. If this was fully converted into radiation, as each photon carries 17.44 keV = $2.79 \cdot 10^{-15}$ J of energy, we expect un upper limit theoretical flux of $4.48 \cdot 10^{17}$ photons per second. We do not know the quantum efficiency of our fine-focus X-ray sealed tube, but we expect it is of the order of 1 %, of which only ~6.6 % will belong to the characteristic Kα fuorescence line. Another factor of ~0.007 comes from ratio between the area of the Be window and the whole solid angle. Considering a further reduction of ~ 1/100 due to monochromator, collimator and air, a cautious total factor of $3.57 \cdot 10^{-9}$ could be employed to account for all the energy losses. This leaves out a flux of $1.60 \cdot 10^{9}$ photons/s, corresponding to a total of $4.32 \cdot 10^{15}$ photons possibly able to interact with the sample over the whole period of 750 hrs of exposure to X-rays. As the μR factor reads 0.081 (Table 1 in the main text), the amount of absorbed radiation is $1-e^{-0.081}$ and the total amount of energy transferred to the crystal should be of the order of 0.9 J.

As the specimen is a sphere with a diameter of 0.5 mm, the total volume is $6.54 \cdot 10^{-5}$ cm^3, corresponding to a mass of $9.43 \cdot 10^{-8}$ kg owing the X-ray estimated density of 1.441 g·cm^{-3}. Finally, the amount of absorbed dose in Grays (Gy) is 0.9 J / $9.43 \cdot 10^{-8}$ kg = 9.5 MGy. For X-rays, we expect that the amount of effective dose, that is, the dose able to cause damage, be equal to the absorbed one.

S5. Crystal packing

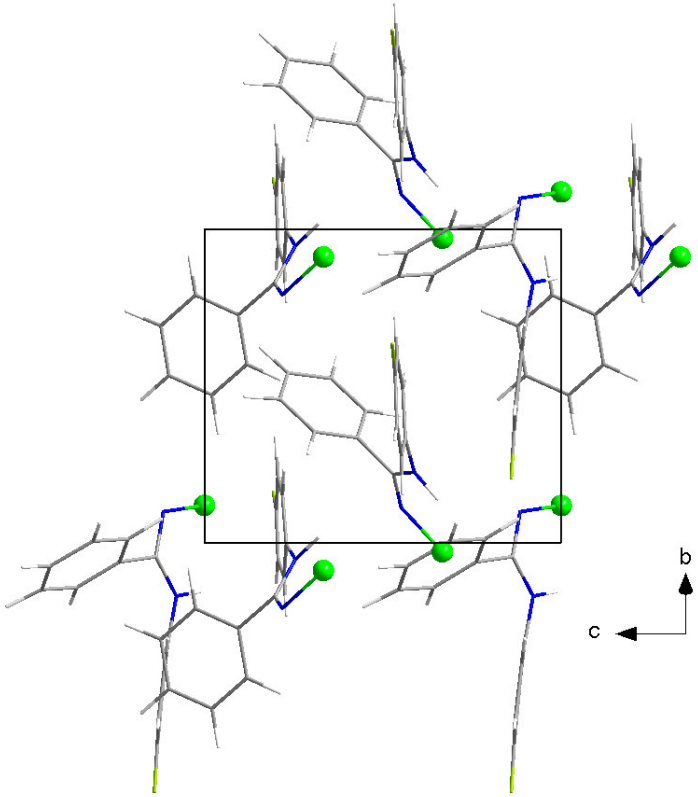

Figure S1. Wires-stick model of NCLBA crystal packing along the *a* axis. Molecules wrap along *c* around the 3_1 screw, setting up a helix motif where chlorine atoms (green spheres) are allocated in the free space between neighboring molecules.

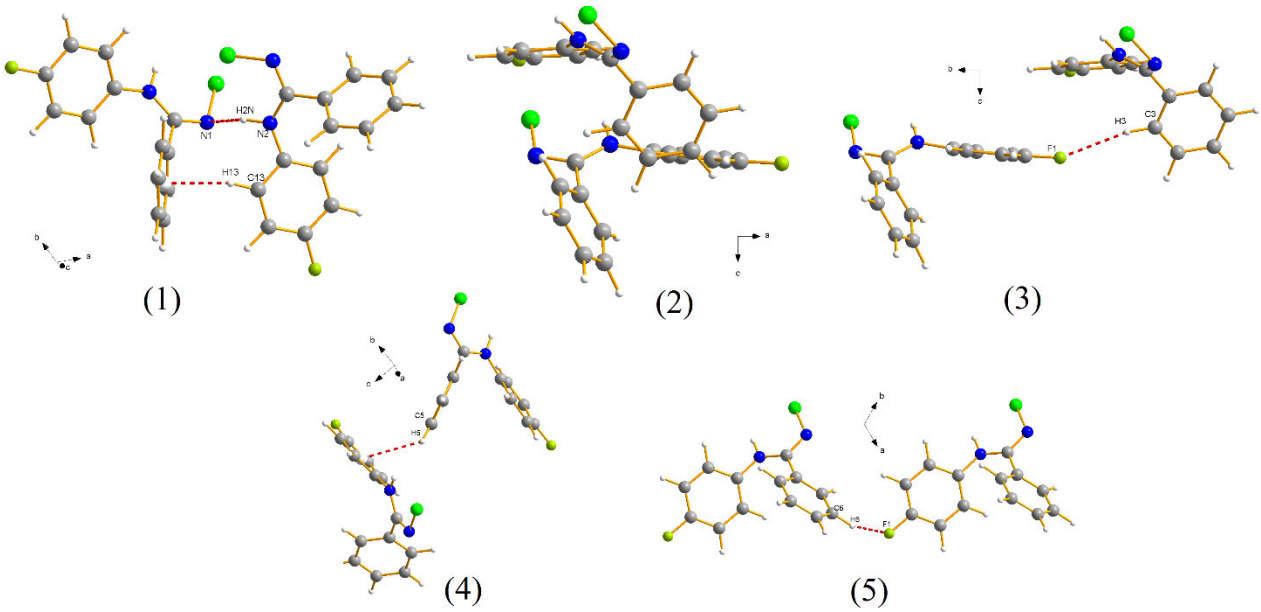

Figure S2. Ball-and-stick representations of molecular pairs shown in Table 2, from the most to the least negative interaction energy (see main text and Table 2 for numbering). H···Acceptor contacts are highlighted as red dashed lines.

S6. Results of multipole refinements

Table S1. Results of the multipolar refinement of NCLBA with VALRAY2000. l_{max} is the maximum order of the multipole expansion; C_{ijk} and D_{ijkl} signal that the Gram-Charlier third and fourth order cumulants are also active in the least-squares (l.s.) refinement.

Model	A C,N,F,Cl: l_{max}=3 H: l_{max}=2	B C,N,F,Cl: l_{max}=4 H: l_{max}=2	C Model B + C_{ijk}(Cl)	D Model C + D_{ijkl} (Cl)	E[(a)] Model B+ C_{ijk} + D_{ijkl} (Cl,F)
Scale factor	1.0065(9)	1.004(1)	1.004(1)	1.003(1)	1.000(2)
Extin. coeff. g_{11}	0.177(7)	0.163(7)	0.164 (7)	0.159(7)	0.161(8)
N. variables (N_v)	517	670	680	695	680
N_{obs}/ N_v	27.7	21.4	21.0	20.6	21.0
On all 14309 observed (I>0) data					
$\sum w\Delta^2$	14060.8796	13375.6562	13312.0334	13115.7719	12695.6271
G.o.f.	1.0097	0.9903	0.9883	0.9815	0.9652
R(F), R(F^2)	0.0165, 0.0195	0.0162, 0.0189	0.0162, 0.0188	0.0161, 0.0187	0.0159, 0.0177
$R_w(F^2)$	0.0289	0.0281	0.0281	0.0279	0.0274
On 402 data with $(\sin\theta/\lambda) \leq 0.35$ (low-angle data)					
R(F), R(F^2)	0.0055, 0.0115	0.0052, 0.0110	0.0052, 0.0110	0.0051, 0.0107	0.0041, 0.0085
$R_w(F^2)$	0.0136	0.0128	0.0128	0.0127	0.0101
On 2625 data with $(\sin\theta/\lambda) \leq 0.35$ (i.e. within the Cu sphere)					
R(F), R(F^2)	0.0079, 0.0135	0.0075, 0.0129	0.0075, 0.0128	0.0074, 0.0126	0.0069, 0.0111
$R_w(F^2)$	0.0183	0.0171	0.0171	0.0169	0.0159
On 11684 data with $0.65 \leq (\sin\theta/\lambda) \leq 1.15$ (high-angle data)					
R(F), R(F^2)	0.0209, 0.0271	0.0207, 0.0264	0.0207, 0.0264	0.0206, 0.0262	0.0205, 0.0259
$R_w(F^2)$	0.0343	0.0337	0.0336	0.0334	0.0331
On 13437 data with $I > 3\sigma(I)$					
Scale factor	1.007(1)	1.005(1)	1.005(1)	1.003(1)	1.000(2)
Extin. coeff. g_{11}	0.178(7)	0.164(7)	0.165(7)	0.159(7)	0.161(9)
$\sum w\Delta^2$	13458.2806	12774.7585	12714.6099	12515.3106	12102.4548
G.o.f.	1.0206	1.0003	0.9983	0.9911	0.9740
R(F), R(F^2)	0.0144, 0.0191	0.0141, 0.0185	0.0141, 0.0184	0.0140, 0.0182	0.0137, 0.0173
$R_w(F^2)$	0.0282	0.0275	0.0274	0.0272	0.0268
N_{obs}/ N_v	26.0	20.1	19.8	19.3	20.1
$\Delta\rho$ min (e Å^{-3})	-0.3373	-0.2763	-0.2727	-0.2698	-0.2478
At X,Y,Z	0.127, 0.162, -0.016	-0.100, -0.400, 0.126	-0.100, -0.400, 0.126	-0.100, -0.400, 0.126	0.151, 0.262, 0.016
$\Delta\rho$ max (e Å^{-3})	0.5095	0.3329	0.2835	0.3031	0.2575
At X,Y,Z	0.127, 0.162, 0.028	0.123, 0.155, 0.030	-0.219, 0.162, 0.097	-0.223, 0.155, 0.094	-0.223, 0.154, 0.093

(a) Includes 10 radial parameters to be refined; C_{ijk} and D_{ijkl} of halogen atoms kept at the values obtained after their previous l.s. refinement.

Table S2. Final geometric and multipole parameters retrieved from model "E" (Table S1).

Box 1: atom specie, atom number, crystallographic coordinates / six U_{ij} tensor elements in the following order: U_{11}, U_{22}, U_{33}, U_{12}, U_{13}, U_{23} (note that the order of the off-diagonal elements is reversed with respect to the standard shelx notation)

```
SCALE   1.000443   1           4
ATOM   CL 01   0.089013  0.118406  0.000000                       0
UIJ    CL 01   0.006344  0.005217  0.007368  0.003193 -0.000429  0.000692
ATOM   F  01  -0.160927 -0.794176  0.140331                       0
UIJ    F  01   0.013114  0.004179  0.016161  0.004909  0.002581  0.002873
ATOM   N  01   0.209995  0.098324  0.115595                       0
UIJ    N  01   0.006229  0.004153  0.007640  0.002176 -0.001386  0.000021
ATOM   N  02   0.053783 -0.170978  0.078869                       0
UIJ    N  02   0.006778  0.003780  0.009682  0.002141 -0.003751 -0.000549
ATOM   C  01   0.172367 -0.044991  0.136584                       0
UIJ    C  01   0.004639  0.004051  0.005792  0.001979 -0.000816 -0.000191
ATOM   C  02   0.272930 -0.061649  0.238114                       0
UIJ    C  02   0.004554  0.005236  0.005210  0.002164 -0.000473  0.000191
ATOM   C  03   0.210421 -0.143198  0.358411                       0
UIJ    C  03   0.005177  0.007102  0.005741  0.002137  0.000101  0.000858
ATOM   C  04   0.308218 -0.149467  0.455553                       0
UIJ    C  04   0.007300  0.007983  0.005962  0.003113 -0.000276  0.001384
ATOM   C  05   0.467106 -0.074594  0.432856                       0
UIJ    C  05   0.006969  0.008615  0.006982  0.004164 -0.001172  0.000612
ATOM   C  06   0.528832  0.004856  0.312118                       0
UIJ    C  06   0.005220  0.008653  0.007429  0.003484 -0.000327  0.000603
ATOM   C  07   0.431602  0.011242  0.214466                       0
UIJ    C  07   0.004848  0.007387  0.006205  0.002614  0.000137  0.001087
ATOM   C  08   0.005815 -0.328214  0.103924                       0
UIJ    C  08   0.005518  0.004116  0.007289  0.002392 -0.001165 -0.000194
ATOM   C  09   0.108419 -0.384318  0.110701                       0
UIJ    C  09   0.005951  0.005365  0.008785  0.003097 -0.000219 -0.000251
ATOM   C  010  0.051902 -0.542012  0.127067                       0
UIJ    C  010  0.007242  0.005991  0.009504  0.004223  0.000599  0.000486
ATOM   C  011 -0.106276 -0.640499  0.132155                       0
UIJ    C  011  0.007755  0.004742  0.008732  0.003429  0.001266  0.001143
ATOM   C  012 -0.210227 -0.587647  0.127455                       0
UIJ    C  012  0.006353  0.004961  0.012674  0.002501  0.000552  0.001084
ATOM   C  013 -0.152639 -0.429736  0.114630                       0
UIJ    C  013  0.005666  0.004916  0.011492  0.002688 -0.000771  0.000469
ATOM   HH 03   0.087910 -0.195190  0.375840                       0
UIJ    HH 03   0.011540  0.027490  0.022670  0.006550  0.002500  0.004690
ATOM   HH 04   0.261490 -0.204300  0.553500                       0
UIJ    HH 04   0.023070  0.029780  0.014970  0.009980  0.002850  0.008300
ATOM   HH 05   0.542960 -0.078300  0.509220                       0
UIJ    HH 05   0.020430  0.030330  0.020050  0.013800 -0.006250  0.002960
ATOM   HH 06   0.651200  0.060410  0.294370                       0
UIJ    HH 06   0.011330  0.030610  0.025610  0.008530  0.001330  0.004030
ATOM   HH 07   0.479520  0.074300  0.121750                       0
UIJ    HH 07   0.018700  0.026630  0.016900  0.008700  0.003960  0.008680
ATOM   HH 09   0.230980 -0.308120  0.102840                       0
UIJ    HH 09   0.011610  0.017010  0.036170  0.005120  0.000580  0.000760
ATOM   HH 010  0.126800 -0.590660  0.131650                       0
UIJ    HH 010  0.020090  0.019790  0.037350  0.014760  0.001330  0.001220
ATOM   HH 012 -0.333690 -0.661900  0.133580                       0
UIJ    HH 012  0.012340  0.016450  0.043930  0.004150  0.002730  0.003100
ATOM   HH 013 -0.228850 -0.384140  0.110880                       0
UIJ    HH 013  0.016400  0.018380  0.039970  0.011890 -0.001810  0.001040
ATOM   HH 02N -0.016150 -0.155980  0.014100                       0
UIJ    HH 02N  0.017970  0.014720  0.021870  0.008250 -0.007680  0.000600
```

Box 2: for each atom, multipole coefficients in the following order: inner/intermediate/outer core spherical population, 3 dipoles, 5 quadrupoles, 7 octupoles (non-H only), 9 hexadecapoles (non-H only). Coefficients are organized as follows, "Y_{lm}" being the corresponding spherical harmonic function (see Table 1 of the Valray users' manual). Dipoles: Y_{11+}, Y_{11-}, Y_{10}. Quadrupoles: Y_{22+}, Y_{22-}, Y_{21+}, Y_{21-}, Y_{20}. Octupoles: Y_{33+}, Y_{33-}, Y_{32+}, Y_{32-}, Y_{31+}, Y_{31-}, Y_{30}. Hexadecapoles: Y_{44+}, Y_{44-}, Y_{43+}, Y_{43-}, Y_{42+}, Y_{42-}, Y_{41+}, Y_{41-}, Y_{40}.

```
POPVAL CL  1   0  1  1.966  2  7.928  3  7.371  4 -0.093  5  0.010  6 -0.083
POPVAL CL  1   1  7 -0.173  8  0.059  9 -0.550 10  0.052 11 -0.210 12 -0.032
POPVAL CL  1   2 13 -0.501 14  0.767 15 -0.157 16  0.215 17 -0.037 18 -0.162
POPVAL CL  1   3 19  0.520 20 -0.943 21 -2.512 22 -2.397 23  0.547 24 -0.216
POPVAL CL  1   4 25  0.087 26 -0.046 27 -0.209
POPVAL F   1   0  1  1.966  2  0.000  3  7.049  4 -0.043  5  0.052  6  0.050
POPVAL F   1   1  7  0.023  8 -0.078  9  0.157 10 -0.003 11  0.001 12 -0.002
POPVAL F   1   2 13 -0.047 14  0.009 15 -0.005 16  0.008 17 -0.020 18  0.007
POPVAL F   1   3 19  0.012 20  0.038 21 -0.122 22 -0.045 23  0.013 24  0.023
POPVAL F   1   4 25 -0.004 26 -0.015 27 -0.005
POPVAL N   1   0  1  1.966  2  0.000  3  5.056  4  0.184  5  0.270  6  0.207
POPVAL N   1   1  7 -0.192  8  0.063  9 -0.290 10  0.005 11 -0.222 12 -0.163
POPVAL N   1   2 13  0.057 14 -0.604 15  1.021 16 -0.091 17  0.083 18  0.039
POPVAL N   1   3 19  0.099 20  0.824 21 -0.803 22 -0.293 23 -0.037 24  0.120
POPVAL N   1   4 25 -0.014 26 -0.045 27 -0.020
POPVAL N   2   0  1  1.966  2  0.000  3  5.095  4 -0.062  5 -0.010  6  0.055
POPVAL N   2   1  7  0.073  8  0.027  9 -0.072 10  0.027 11  0.053 12 -0.357
POPVAL N   2   2 13  0.209 14 -1.105 15  0.988 16 -0.142 17  0.139 18 -0.056
POPVAL N   2   3 19  0.076 20 -0.223 21 -0.737 22 -0.593 23  0.053 24  0.239
POPVAL N   2   4 25 -0.162 26  0.037 27 -0.024
POPVAL C   1   0  1  1.966  2  0.000  3  4.117  4 -0.057  5  0.083  6  0.096
POPVAL C   1   1  7 -0.405  8 -0.577  9  1.631 10 -0.043 11 -0.608 12  1.642
POPVAL C   1   2 13 -0.846 14  6.050 15 -4.318 16  0.885 17 -0.526 18  0.517
POPVAL C   1   3 19  0.310 20  2.332 21 -5.847 22  0.590 23 -0.081 24  0.328
POPVAL C   1   4 25 -0.385 26  0.781 27 -0.523
POPVAL C   2   0  1  1.966  2  0.000  3  4.201  4  0.159  5 -0.139  6  0.124
POPVAL C   2   1  7  0.324  8  0.812  9 -0.031 10 -1.055 11  0.300 12 -0.055
POPVAL C   2   2 13  0.585 14 -2.937 15  0.450 16 -1.240 17 -0.699 18  0.270
POPVAL C   2   3 19 -1.761 20  4.065 21  0.905 22 -3.653 23 -0.374 24 -0.143
POPVAL C   2   4 25  0.644 26 -1.098 27 -0.513
POPVAL C   3   0  1  1.966  2  0.000  3  4.025  4  0.144  5 -0.050  6  0.061
POPVAL C   3   1  7  0.615  8  0.934  9  0.730 10 -1.084 11  0.177 12  0.283
POPVAL C   3   2 13 -1.737 14  4.010 15  0.974 16  1.144 17  0.743 18 -0.681
POPVAL C   3   3 19 -0.427 20  1.223 21  1.743 22 -0.334 23  0.821 24 -0.887
POPVAL C   3   4 25  0.085 26  0.861 27  0.171
POPVAL C   4   0  1  1.966  2  0.000  3  3.999  4  0.098  5 -0.047  6  0.074
POPVAL C   4   1  7  0.494  8  0.894  9  0.533 10 -1.228 11 -0.021 12  0.116
POPVAL C   4   2 13  0.704 14 -2.970 15  0.632 16 -1.086 17 -1.078 18  0.522
POPVAL C   4   3 19 -1.153 20 -1.133 21 -0.805 22  0.500 23 -1.301 24 -0.631
POPVAL C   4   4 25  0.799 26 -0.119 27 -0.741
POPVAL C   5   0  1  1.966  2  0.000  3  4.075  4  0.041  5 -0.100  6 -0.053
POPVAL C   5   1  7  0.406  8  1.073  9  0.506 10 -1.137 11  0.253 12  0.373
POPVAL C   5   2 13 -1.116 14  4.225 15 -0.022 16  1.318 17  0.731 18 -0.813
POPVAL C   5   3 19 -1.531 20  5.199 21 -2.107 22  2.561 23  0.008 24 -0.892
POPVAL C   5   4 25 -0.754 26 -0.364 27  0.474
POPVAL C   6   0  1  1.966  2  0.000  3  4.061  4  0.103  5  0.055  6  0.062
POPVAL C   6   1  7  0.374  8  0.987  9  0.606 10 -1.121 11  0.550 12 -0.202
POPVAL C   6   2 13  1.314 14 -2.822 15 -1.115 16 -1.206 17 -0.693 18  0.481
POPVAL C   6   3 19 -0.636 20  2.742 21  0.233 22 -2.796 23 -0.744 24  0.454
POPVAL C   6   4 25  1.111 26 -0.741 27 -1.434
POPVAL C   7   0  1  1.966  2  0.000  3  4.066  4  0.011  5 -0.263  6  0.148
POPVAL C   7   1  7  0.418  8  0.687  9  0.738 10 -1.009 11  0.258 12 -0.004
POPVAL C   7   2 13 -1.010 14  3.310 15 -1.042 16  1.336 17  1.030 18 -0.647
POPVAL C   7   3 19 -0.193 20  0.747 21  0.355 22 -3.941 23 -0.090 24  1.600
POPVAL C   7   4 25 -1.126 26 -1.340 27 -1.349
POPVAL C   8   0  1  1.966  2  0.000  3  4.039  4 -0.098  5 -0.393  6  0.185
POPVAL C   8   1  7  0.395  8  0.219  9  0.118 10 -0.251 11 -1.301 12  0.985
POPVAL C   8   2 13 -2.625 14  0.832 15  1.689 16  0.320 17 -0.179 18  0.028
POPVAL C   8   3 19  0.931 20  1.833 21 -3.839 22  0.864 23  0.008 24 -0.210
POPVAL C   8   4 25  0.533 26 -0.994 27  0.274
POPVAL C   9   0  1  1.966  2  0.000  3  4.012  4 -0.158  5 -0.163  6  0.096
POPVAL C   9   1  7 -0.045  8 -0.086  9 -0.082 10 -0.480 11 -1.298 12 -1.301
POPVAL C   9   2 13  2.274 14 -0.654 15  1.239 16 -0.021 17 -0.158 18 -0.069
POPVAL C   9   3 19 -0.007 20  2.711 21 -2.338 22 -0.676 23 -0.402 24  0.673
POPVAL C   9   4 25 -1.113 26  0.586 27  0.468
POPVAL C   10  0  1  1.966  2  0.000  3  4.026  4 -0.193  5 -0.042  6  0.015
POPVAL C   10  1  7  0.104  8  0.148  9 -0.079 10 -0.328 11 -1.544 12  0.761
```

Table S2, box 2 continued

```
POPVAL C   10  2 13 -2.765 14  0.041 15  1.989 16 -0.240 17  0.427 18  0.069
POPVAL C   10  3 19 -0.185 20  1.310 21 -4.909 22 -3.914 23 -0.227 24  0.684
POPVAL C   10  4 25 -0.493 26  0.025 27  1.672
POPVAL C   11  0  1  1.966  2  0.000  3  4.110  4 -0.086  5  0.322  6 -0.008
POPVAL C   11  1  7  0.769  8  0.264  9  0.004 10  0.097 11 -1.194 12 -1.475
POPVAL C   11  2 13  2.626 14 -0.232 15 -0.793 16  0.325 17  0.609 18 -0.271
POPVAL C   11  3 19  1.532 20  6.286 21 -3.035 22 -1.629 23  0.456 24  1.285
POPVAL C   11  4 25 -0.110 26 -1.064 27  0.472
POPVAL C   12  0  1  1.966  2  0.000  3  4.002  4 -0.015  5  0.047  6 -0.081
POPVAL C   12  1  7 -0.076  8  0.127  9  0.032 10 -0.136 11 -1.114 12  1.138
POPVAL C   12  2 13 -2.525 14  0.827 15  1.533 16  0.268 17  0.334 18 -0.075
POPVAL C   12  3 19 -0.142 20 -2.342 21 -2.430 22 -2.381 23  0.325 24 -1.339
POPVAL C   12  4 25  0.960 26  2.146 27 -0.796
POPVAL C   13  0  1  1.966  2  0.000  3  4.082  4  0.000  5 -0.263  6  0.089
POPVAL C   13  1  7 -0.049  8 -0.002  9 -0.026 10 -0.495 11 -1.354 12 -1.169
POPVAL C   13  2 13  2.295 14 -1.062 15  0.676 16  0.237 17  0.048 18 -0.182
POPVAL C   13  3 19 -0.119 20  3.339 21 -1.076 22 -3.635 23 -0.723 24  0.308
POPVAL C   13  4 25 -0.955 26 -0.412 27  0.516
POPVAL HH  3   0  1  0.000  2  0.000  3  0.919  4  0.521  5  0.123  6 -0.141
POPVAL HH  3   1  7  0.616  8  0.804  9 -0.387 10 -0.316 11 -0.610 12  0.000
POPVAL HH  3   2 13  0.000 14  0.000 15  0.000 16  0.000 17  0.000 18  0.000
POPVAL HH  3   3 19  0.000 20  0.000 21  0.000 22  0.000 23  0.000 24  0.000
POPVAL HH  3   4 25  0.000 26  0.000 27  0.000
POPVAL HH  4   0  1  0.000  2  0.000  3  0.909  4  0.259  5 -0.053  6 -0.804
POPVAL HH  4   1  7 -0.030  8  0.974  9 -0.045 10 -0.361 11  0.909 12  0.000
POPVAL HH  4   2 13  0.000 14  0.000 15  0.000 16  0.000 17  0.000 18  0.000
POPVAL HH  4   3 19  0.000 20  0.000 21  0.000 22  0.000 23  0.000 24  0.000
POPVAL HH  4   4 25  0.000 26  0.000 27  0.000
POPVAL HH  5   0  1  0.000  2  0.000  3  0.952  4 -0.482  5  0.006  6 -0.306
POPVAL HH  5   1  7  0.314  8 -0.989  9  1.257 10 -0.884 11 -0.486 12  0.000
POPVAL HH  5   2 13  0.000 14  0.000 15  0.000 16  0.000 17  0.000 18  0.000
POPVAL HH  5   3 19  0.000 20  0.000 21  0.000 22  0.000 23  0.000 24  0.000
POPVAL HH  5   4 25  0.000 26  0.000 27  0.000
POPVAL HH  6   0  1  0.000  2  0.000  3  0.944  4 -0.402  5 -0.216  6  0.248
POPVAL HH  6   1  7 -0.043  8  0.200  9 -0.078 10 -0.033 11 -0.457 12  0.000
POPVAL HH  6   2 13  0.000 14  0.000 15  0.000 16  0.000 17  0.000 18  0.000
POPVAL HH  6   3 19  0.000 20  0.000 21  0.000 22  0.000 23  0.000 24  0.000
POPVAL HH  6   4 25  0.000 26  0.000 27  0.000
POPVAL HH  7   0  1  0.000  2  0.000  3  0.968  4 -0.251  5 -0.543  6  0.501
POPVAL HH  7   1  7 -0.279  8  0.092  9 -1.222 10 -0.574 11  1.201 12  0.000
POPVAL HH  7   2 13  0.000 14  0.000 15  0.000 16  0.000 17  0.000 18  0.000
POPVAL HH  7   3 19  0.000 20  0.000 21  0.000 22  0.000 23  0.000 24  0.000
POPVAL HH  7   4 25  0.000 26  0.000 27  0.000
POPVAL HH  9   0  1  0.000  2  0.000  3  0.944  4 -0.674  5 -0.428  6 -0.187
POPVAL HH  9   1  7  0.186  8 -0.077  9  0.836 10  0.349 11 -0.903 12  0.000
POPVAL HH  9   2 13  0.000 14  0.000 15  0.000 16  0.000 17  0.000 18  0.000
POPVAL HH  9   3 19  0.000 20  0.000 21  0.000 22  0.000 23  0.000 24  0.000
POPVAL HH  9   4 25  0.000 26  0.000 27  0.000
POPVAL HH  10  0  1  0.000  2  0.000  3  0.902  4 -0.431  5  0.371  6 -0.091
POPVAL HH  10  1  7  0.389  8 -1.173  9 -0.039 10  1.017 11 -0.357 12  0.000
POPVAL HH  10  2 13  0.000 14  0.000 15  0.000 16  0.000 17  0.000 18  0.000
POPVAL HH  10  3 19  0.000 20  0.000 21  0.000 22  0.000 23  0.000 24  0.000
POPVAL HH  10  4 25  0.000 26  0.000 27  0.000
POPVAL HH  12  0  1  0.000  2  0.000  3  0.946  4  0.695  5 -0.006  6 -0.019
POPVAL HH  12  1  7  0.209  8  1.015  9  0.068 10 -0.451 11 -0.424 12  0.000
POPVAL HH  12  2 13  0.000 14  0.000 15  0.000 16  0.000 17  0.000 18  0.000
POPVAL HH  12  3 19  0.000 20  0.000 21  0.000 22  0.000 23  0.000 24  0.000
POPVAL HH  12  4 25  0.000 26  0.000 27  0.000
POPVAL HH  13  0  1  0.000  2  0.000  3  0.968  4  0.608  5 -0.201  6  0.153
POPVAL HH  13  1  7  0.255  8 -0.711  9  0.304 10  0.404 11 -0.550 12  0.000
POPVAL HH  13  2 13  0.000 14  0.000 15  0.000 16  0.000 17  0.000 18  0.000
POPVAL HH  13  3 19  0.000 20  0.000 21  0.000 22  0.000 23  0.000 24  0.000
POPVAL HH  13  4 25  0.000 26  0.000 27  0.000
POPVAL HH  2N  0  1  0.000  2  0.000  3  0.754  4  0.543  5  0.055  6  0.337
POPVAL HH  2N  1  7  0.503  8 -0.488  9  0.615 10  0.392 11 -0.061 12  0.000
POPVAL HH  2N  2 13  0.000 14  0.000 15  0.000 16  0.000 17  0.000 18  0.000
POPVAL HH  2N  3 19  0.000 20  0.000 21  0.000 22  0.000 23  0.000 24  0.000
POPVAL HH  2N  4 25  0.000 26  0.000 27  0.000
```

Box 3: For each atom, radial parameters ($Å^{-1}$) from $l = 0$ to $l = 4$

```
RADPRM CL  1        1.005 0 3 3.610 2 1 3.610 2 1 3.610 3 1 3.610 4 1
RADPRM F   1        0.994 0 3 5.777 2 1 5.777 2 1 5.777 3 1 5.777 4 1
RADPRM N   1        0.985 0 3 3.950 2 1 3.950 2 1 3.950 3 1 3.950 4 1
RADPRM N   2        0.985 0 3 3.950 2 1 3.950 2 1 3.950 3 1 3.950 4 1
RADPRM C   1        0.996 0 3 2.961 2 1 2.961 2 1 2.961 3 1 2.961 4 1
RADPRM C   2        0.996 0 3 2.961 2 1 2.961 2 1 2.961 3 1 2.961 4 1
RADPRM C   3        0.996 0 3 2.961 2 1 2.961 2 1 2.961 3 1 2.961 4 1
RADPRM C   4        0.996 0 3 2.961 2 1 2.961 2 1 2.961 3 1 2.961 4 1
RADPRM C   5        0.996 0 3 2.961 2 1 2.961 2 1 2.961 3 1 2.961 4 1
RADPRM C   6        0.996 0 3 2.961 2 1 2.961 2 1 2.961 3 1 2.961 4 1
RADPRM C   7        0.996 0 3 2.961 2 1 2.961 2 1 2.961 3 1 2.961 4 1
RADPRM C   8        0.996 0 3 2.961 2 1 2.961 2 1 2.961 3 1 2.961 4 1
RADPRM C   9        0.996 0 3 2.961 2 1 2.961 2 1 2.961 3 1 2.961 4 1
RADPRM C   10       0.996 0 3 2.961 2 1 2.961 2 1 2.961 3 1 2.961 4 1
RADPRM C   11       0.996 0 3 2.961 2 1 2.961 2 1 2.961 3 1 2.961 4 1
RADPRM C   12       0.996 0 3 2.961 2 1 2.961 2 1 2.961 3 1 2.961 4 1
RADPRM C   13       0.996 0 3 2.961 2 1 2.961 2 1 2.961 3 1 2.961 4 1
RADPRM HH  3        2.259 0 1 2.259 1 1 2.259 2 1
RADPRM HH  4        2.259 0 1 2.259 1 1 2.259 2 1
RADPRM HH  5        2.259 0 1 2.259 1 1 2.259 2 1
RADPRM HH  6        2.259 0 1 2.259 1 1 2.259 2 1
RADPRM HH  7        2.259 0 1 2.259 1 1 2.259 2 1
RADPRM HH  9        2.259 0 1 2.259 1 1 2.259 2 1
RADPRM HH  10       2.259 0 1 2.259 1 1 2.259 2 1
RADPRM HH  12       2.259 0 1 2.259 1 1 2.259 2 1
RADPRM HH  13       2.259 0 1 2.259 1 1 2.259 2 1
RADPRM HH  2N       2.405 0 1 2.405 1 1 2.405 2 1
```

Box 4: high order cumulants ($x\ 10^4$) on Cl and F as follows. 3rd order: C_{111}, C_{112}, C_{122}, C_{113}, C_{123}, C_{133}, C_{222}, C_{223}, C_{233}, C_{333}; 4th order: D_{1111}, D_{1112}, D_{1122}, D_{1113}, D_{1123}, D_{1133}, D_{1222}, D_{1223}, D_{1233}, D_{1333}, D_{2222}, D_{2223}, D_{2233}, D_{2333}, D_{3333}.

```
CUMCOF CL  1  4     0.00024    -0.00869    -0.01700     0.01241     0.06060
CUMCOF             -0.00680    -0.01837     0.03570     0.00169     0.01507
CUMCOF              0.00080    -0.00030    -0.00131    -0.00115     0.00346
CUMCOF              0.00515    -0.00292     0.00859     0.00343     0.00005
CUMCOF             -0.00118     0.00244     0.00434     0.00100     0.00096
CUMCOF F   1  4     0.00785    -0.07838    -0.14336    -0.01212     0.12579
CUMCOF              0.08770    -0.14450     0.02494     0.03217    -0.05392
CUMCOF              0.01471     0.02535     0.02052    -0.01434    -0.00782
CUMCOF              0.02139     0.00697    -0.00083     0.01793    -0.00691
CUMCOF             -0.00368     0.00499     0.00337     0.00611     0.00584
```

S7. Bond lengths

S7.1 Experimental and theoretical geometries and convergence of the basis set

The pob-TZVP-rev2 triple-zeta valence + polarization basis set designed by Peintinger, Oliveira and Bredow for the computation of solid-state systems,[7,8] combined with the PBE0 hybrid density functional,[9] was used to calculate the equilibrium crystalline geometry of NCLBA with the code CRYSTAL17.[10] The most relevant geometric parameter is undoubtedly the length of the N-Cl bond, whose value could be closely related to the well-known lability of the bond itself. The calculated value of this parameter, 1.816 Å, overestimates the experimental value by 0.067 Å (3.8%). In order to explain this discrepancy, it may be useful to study the convergence properties of the basis set with respect to the value of $R_{N\text{-}CL}$. As this cannot be done by periodic ab initio methods due to the excessive computational effort required, we focused on computation of the equilibrium geometry and electrostatic properties of the NCLBA molecule in vacuum. The pob-TZVP-rev2 basis set is based on the def2-TZVP basis set developed for molecules by the Ahlrichs group.[11] For this reason and in order to consistently and reliably compare the equilibrium geometries of NCLBA in the solid state and in the vacuum, the equilibrium geometry and dipole moment of the NCLBA molecule in vacuum were calculated using the def2-TZVP basis set together with the PBE0 density functional.

Table S3 - N-Cl equilibrium distance and dipole moment for the N-chloro-N'-(4-fluoro-phenyl)-benzamidine (NCLBA) molecule in vacuum.

basis set		M¶	density functional			
			PBE0		B3LYP	
			$R_{N\text{-}Cl}$ (Å)	μ (D)	$R_{N\text{-}Cl}$ (Å)	μ (D)
A5	def2-aug-TZVPP	1321	1.7219	2.338	1.7545	2.422
A4	def2-aug-TZVPP(-f)	1083	1.7322	2.458	1.7652	2.544
A3	def2-TZVP	879	1.7224	2.338	1.7545	2.387
A2	def2-TZVP(-f)	760	1.7335	2.376	1.7670	2.439
A1	pob-TZVP-rev2	651	1.8052	2.484	1.8398	2.530
B5	6-311++G(3df,3pd)	1101	1.7205	2.346	1.7514	2.400
B4	6-311G(3df,3pd)	1023	1.7220	2.534	1.7543	2.635
B3	6-311++G(2d,2p)	817	1.7405	2.457	1.7330	2.529
B2	6-311G(2d,2p)	739	1.7457	2.712	1.7812	2.833
B1	6-311G(d,p)	624	1.7533	2.741	1.7904	2.868
C1	aug-pc-1	780	1.7571	2.530	1.7914	2.607

¶ Number of primitive gaussian functions.

The convergence properties of the basis set were analyzed by using bases which comprise a different number of primitive functions, such as the pob-TZVP-rev2 itself, the def2-TZVP (-f) which does not contain f functions and the def2-aug-TZVPP which is augmented by diffuse functions and

has 2p1d polarization for hydrogen, together with some of the valence triple-zeta plus polarization Pople basis sets, like 6-311G(d,p) and 6-311++G(2d,2p),[12] and Jensen polarization-consistent basis set, aug-pc-1,[13] which is of double-zeta plus polarization quality augmented by diffuse functions. Calculations were performed with both the PBE0 and the popular B3LYP density functionals.[14–17] The results are summarized in Table S3 and Figures S3-S5, focusing on the equilibrium distance $R_{N\text{-}Cl}$ and the magnitude of the molecular dipole moment.

In addition to the methods reported in Table S3, the B2PLYP double-hybrid functional[18] was also used, combined with the aug-pc-1 basis set, as it was indicated as one of the theoretical models that can provide an excellent compromise between accuracy and computational efficiency in the calculation of molecular dipole moments.[19–21] The calculation yielded a value of $R_{N\text{-}Cl}$ = 1.7901 Å, which is practically identical to those obtained with the B3LYP/6-311G(d,p) and B3LYP/aug-pc-1 models, and a value of the molecular dipole moment μ = 2.885 D that is quite close to the B3LYP/6-311G(d,p) value.

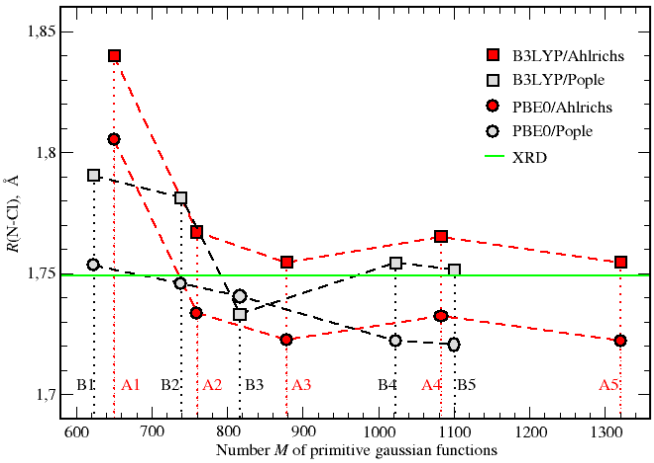

Figure S3. Basis set convergence of equilibrium N-Cl bond length of NCLBA in vacuum for two basis set families (Ahlrichs: red symbols, Pople: grey symbols) and two density functionals (B3LYP: squares, PBE0: circles). For each density functional, the dashed lines connect the points belonging to the same basis set family. Vertical dotted lines mark the individual basis sets (A1: pob-TZVP-rev2, M = 651; A2: def2-TZVP (-f), M = 760; A3: def2-TZVP, M = 879; A4: def2-aug-TZVPP(-f), M = 1083; A5: def2-aug-TZVPP, M = 1321).

As shown in Figure S3, the equilibrium value of $R_{N\text{-}Cl}$ calculated for the NCLBA molecule in vacuum decreases with some oscillations as the number M of the basis functions increases and eventually reaches a constant value. Both Ahlrichs and Pople families of basis functions, combined with the density functional B3LYP, nicely converge towards the experimental value of $R_{N\text{-}Cl}$. The PBE0 values follow the same trend as they are linearly correlated to the B3LYP values, as shown in Figure S4. However, they are sistematically lower than the B3LYP values by the average amount of

ΔR_{av} = 0.0334(16) Å, except in the case of the 6-311++G(2d,2p) values which differ slightly by -0.0075 Å and were not included in the least-squares regression line of Figure S4.

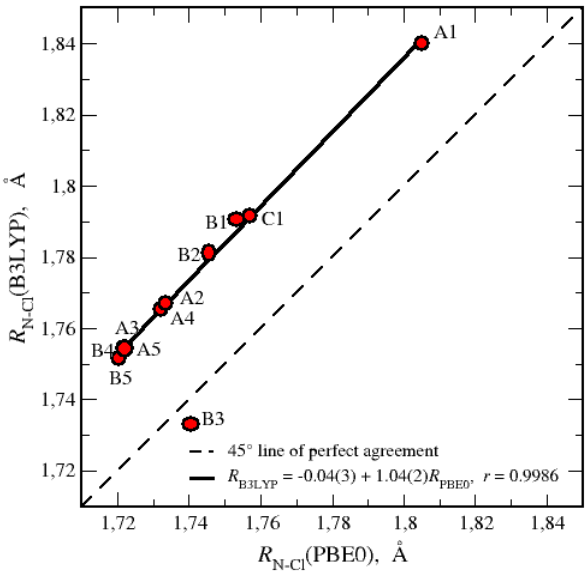

Figure S4. Relationship between B3LYP and PBE0 values of the N-Cl equilibrium distance for the basis sets specified in Table S3. Point B3 is not included in the regression line.

In Table S3 and Figure S3 we monitored the trend of $R_{N\text{-}CL}$ values as a function of the extent M of the basis set. It is clear that for each model (eg PBE0 and B3LYP) and for each family of basis functions (Ahlrichs and Pople) the $R_{N\text{-}CL}$ bond distance tends to a constant value as the size of the basis set increases. This result is not surprising, and it is to be expected that it can be found for all pairs of bonded atoms.

In Table S4, the experimental values (XRD) of the bond lengths in the amidine fragment of NCLBA are compared with the corresponding equilibrium values of the molecule in the crystalline state and in the vacuum, calculated using the functional PBE0 and the basis functions A0 through A5 (with A0 being the periodic equivalent of A1). This is graphically displayed in Figure S5. The linear regression line (red line) shows an almost quantitative agreement (r = 0.9994) between calculated and experimental values, slightly deviating from the 45° line of perfect agreement (dotted line) due to a slope of 0.976 (6). There are only two outliers that correspond to the values calculated with the pob-TZVP-rev2 basis set in the solid state (black circle, periodic PBE0/A0) and in the gas phase (red square, PBE0/A1); these two points were not included in the linear regression.

Table S4. Comparison of the experimental (XRD) geometry of the amidine fragment of NCLBA with the equilibrium geometries calculated in the crystalline state (A0: periodic PBE0/pob-TZVP-rev2) and for the molecule in vacuum (using the PBE0 density functional and the following Ahlrichs basis sets A1: pob-TZVP-rev2, M = 651; A2: def2-TZVP (-f), M = 760; A3: def2-TZVP, M = 879; A4: def2-aug-TZVPP(-f), M = 1083; A5: def2-aug-TZVPP, M = 1321).

	XRD	A0	A1	A2	A3	A4	A5
Bond lengths							
N1-Cl1	1.7490(2)	1.8162	1.8052	1.7335	1.7224	1.7322	1.7220
N1-C1	1.3064(2)	1.3051	1.2989	1.2927	1.2927	1.2923	1.2927
C1-N2	1.3533(2)	1.3478	1.3617	1.3593	1.3588	1.3602	1.3593
C1-C2	1.4893(2)	1.4827	1.4794	1.4822	1.4822	1.4823	1.4821
N2-C8	1.4207(2)	1.4162	1.4120	1.4074	1.4058	1.4108	1.4066
N2-H2N	1.0143(2)	1.0176	1.0152	1.0111	1.0110	1.0103	1.0105
Bond angles							
C1-N1-Cl1	113.24	112.64	112.18	113.96	114.30	113.89	114.25
N1-C1-N2	126.52	127.77	126.21	125.51	125.34	125.79	125.43
N1-C1-C2	112.99	111.46	113.33	114.12	114.21	114.37	114.34
N2-C1-C2	120.47	120.71	120.33	120.20	120.29	119.67	120.10
C1-N2-C8	127.87	128.85	128.32	128.39	128.83	126.86	128.39
C1-N2-H2N	118.50	115.99	113.59	113.34	113.48	113.71	113.58
C8-N2-H2N	113.50	115.13	117.01	116.20	116.19	116.68	116.38
Dihedral angles							
N2-C1-N1-Cl1	0.05	1.14	4.57	4.76	4.45	4.71	4.17
H2N-N2-C1-N1	1.54	0.86	6.62	5.83	7.16	5.05	6.69
C2-C1-N1-Cl1	178.31	178.30	179.63	179.97	179.89	179.99	179.96
C3-C2-C1-N1	118.40	120.94	134.57	135.76	135.69	134.86	134.18
H2N-N2-C8-C9	138.29	138.01	134.91	132.28	134.65	125.29	135.34
Intramolecular short distances							
Cl1-H2N	2.407	2.400	2.312	2.311	2.318	2.323	2.319
C1-C3	2.509	2.493	2.496	2.498	2.499	2.493	2.497
N2-H3	2.978	2.924	2.764	2.746	2.752	2.732	2.765
C8-H3	2.928	2.914	2.773	2.794	2.787	2.803	2.824
C3-N2	3.120	3.081	2.997	2.987	2.991	2.975	2.995
C8-C2	2.985	3.001	3.028	3.039	3.043	3.008	3.031
C3-C8	3.188	3.197	3.143	3.166	3.165	3.146	3.170

The variation coefficient of $R_{\text{N-Cl}}$, calculated for the range of values A2-A5, amounts to 0.31% but increases to 2.26% if the two outliers A0 and A1 are also included. The coefficient of variation relative to the other bond distances reported in Table 2 and calculated for the complete range of values A0-A5, is consistently small: 0.37% (C1-N1), 0.34% (C1-N2), 0.07% (C1-C2), 0.25% (C8-N2), and 0.28% (N2-H2N). These results show that there are no significant differences in the values of the bond lengths passing from the molecule in the crystalline state to the gas phase. The observed discrepancy between the calculated values A0 and A1 and the experimental value of the N-Cl bond length is probably due to the inadequacy of the basis set pob-TZVP-rev2 in describing such a bond. In addition, this basis set, together with the 6-311G(d, p) one, is among the smallest used in our study (M = 651 and 624, respectively).

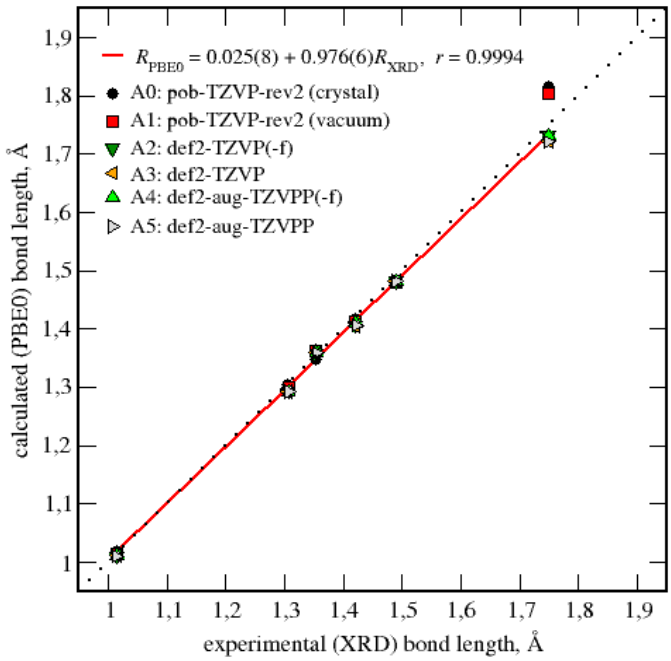

Figure S5. Comparison of the experimental values (XRD) of the bond lengths in the amidine fragment of NCLBA and the corresponding equilibrium values of the molecule in the crystalline state and in the vacuum, calculated using the functional PBE0 and the basis functions A0 through A5. The two values of RN-Cl, calculated for the molecule in the crystal (A0, black circle) and in the vacuum (A1, red square) with the pob-TZVP basis set, are not included in the regression.

Table S5. Comparison of point topological properties at the N–Cl covalent bond in different organic molecules, as obtained from PBE0/pob-TZVP-rev2 and D3-Grimme corrected quantum calculations on gas-phase molecules frozen at their in-crystal geometries. Data of N–Cl in NCLBA are highlighted in bold.

Substance	Bond	Density / e·Å–3	Laplacian / e·Å^{-5}	Ellipt.	Hessian Eigenvalues / e·Å^{-5}			Bond length / Å
					λ_1	λ_2	λ_3	
AZCFOM01	Cl1-N4	1.3129	-2.70062	0.019	-6.814	-6.686	10.799	1.7214
AZCFOM01	Cl6-N9	1.3129	-2.70198	0.019	-6.813	-6.685	10.797	1.7214
ENAJIO	N10-Cl11	1.3781	-3.91452	0.014	-6.948	-6.851	9.885	1.6948
ENAJIO	N26-Cl27	1.3776	-3.90675	0.014	-6.946	-6.849	9.888	1.6950
FEVNUP	Cl1-N10	1.2684	-2.06948	0.012	-6.486	-6.407	10.824	1.7360
GUGREH	Cl1-N3	1.2683	-2.28459	0.023	-6.516	-6.370	10.601	1.7346
NUJJAF	N8-Cl10	1.3497	-3.30437	0.017	-6.981	-6.863	10.540	1.7067
NUXXOV	N5-Cl19	1.2881	-2.52804	0.019	-6.633	-6.512	10.616	1.7286
PASJAV	Cl44-N252	1.3346	-3.23972	0.011	-6.798	-6.723	10.281	1.7099
RAQBIX	N141-Cl16	1.2033	-1.05024	0.016	-6.159	-6.064	11.173	1.7636
SEMHOI	N8-Cl10	1.2870	-2.54446	0.055	-6.625	-6.281	10.361	1.7316
SEMHOI	N8-Cl11	1.2399	-1.81164	0.060	-6.420	-6.057	10.665	1.7500
SEMHOI	N9-Cl12	1.2893	-2.48808	0.011	-6.596	-6.522	10.630	1.7281
TIYDAI	Cl1-N2	1.2976	-2.58558	0.019	-6.696	-6.569	10.680	1.7264
TIYDOW01	Cl1-N8	1.3583	-3.47767	0.017	-6.916	-6.803	10.242	1.7022
TIYDOW02	Cl13-N20	1.3583	-3.47765	0.017	-6.916	-6.803	10.242	1.7022
TIYDOW	N15-Cl16	1.3764	-3.84732	0.017	-6.952	-6.837	9.942	1.6959
TIYDOW	N3-Cl4	1.3764	-3.84701	0.017	-6.952	-6.837	9.942	1.6950
TIYFAK	Cl1-N2	1.2990	-2.60807	0.017	-6.691	-6.577	10.661	1.7259
TUWDIY	Cl1-N3	1.3098	-2.84171	0.017	-6.706	-6.595	10.459	1.7196
XOLYAA	Cl2-N9	1.2995	-2.58249	0.012	-6.696	-6.617	10.731	1.7282
NCLBA QM sp [a]	**Cl1-N2**	**1.2351**	**-1.43495**	**0.021**	**-7.3331**	**-7.2278**	**11.0618**	**1.7490**
NCLBA QM periodic [b]	**Cl1-N2**	**1.2350**	**-1.42000**	**0.020**	**-6.36**	**-6.21**	**11.15**	**1.7490**
NCLBA expt [c]	**CL1-N1**	**1.25(2)**	**5.1(4)**	**0.07(4)**	**-6.5(3)**	**-6.0(3)**	**17.6(2)**	**1.7490(2)**

[a] Single-point calculation on the molecule extracted from the crystal at 17.5 K.
[b] Single-point calculation on the frozen crystal structure.
[c] Multipole refinement against the experimental data. Estimated standard deviations are reported in parentheses.

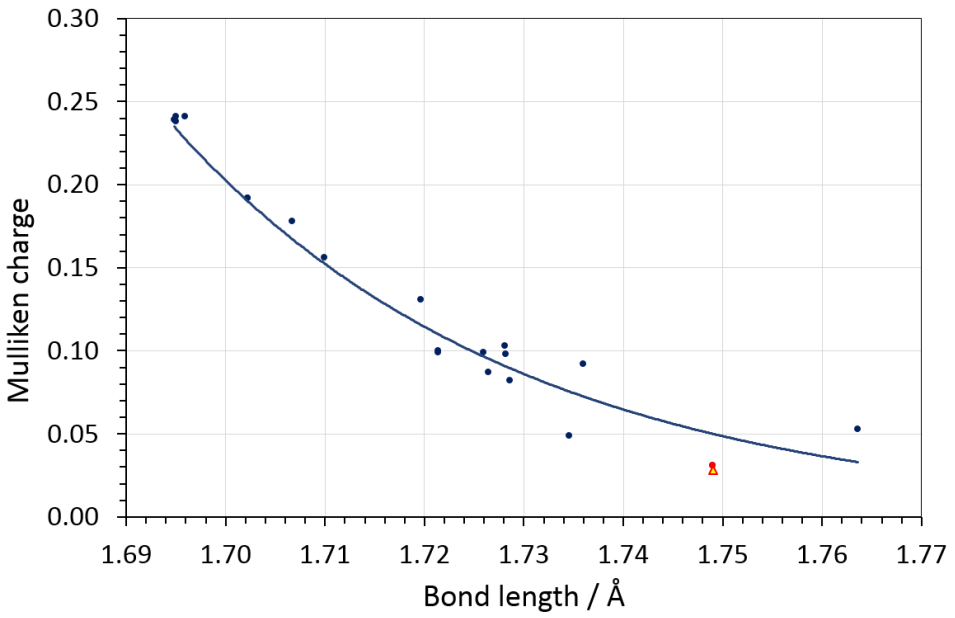

Figure S6. Mulliken net charge of Cl vs. covalent bond length along the series of halogenated imine compounds (Section S2 SI) here considered. Calculations come from D3 Grimme–corrected PBE0 wavefunctions at frozen experimental geometries using a pob-TZVP-rev2 triple-zeta valence + polarization basis set. Full red dot: NCLBA *in vacuo*. Red triangle: NCLBA in the solid-state. The curve has equation $y = 2 \cdot 10^{20} \cdot \exp[-28.54]x$ and comes from a linear exponential fitting against the available data *in vacuo*.

S8. Electrostatic properties

Table S6. Experimental atomic net charges in the NCLBA crystal from Stewart and QTAIM dma

Atom	Stewart	QTAIM
CL1	-0.273 (.029)	-0.194 (.028)
F1	-0.019 (.025)	-0.481 (.024)
N1	-0.025 (.031)	-0.543 (.026)
N2	-0.064 (.043)	-1.057 (.024)
C1	-0.086 (.029)	0.793 (.017)
C2	-0.170 (.034)	-0.204 (.021)
C3	0.006 (.044)	-0.054 (.026)
C4	0.032 (.041)	-0.074 (.024)
C5	-0.044 (.041)	-0.117 (.022)
C6	-0.030 (.041)	-0.046 (.021)
C7	-0.034 (.042)	-0.127 (.023)
C8	-0.008 (.032)	0.238 (.020)
C9	0.020 (.044)	-0.032 (.024)
C10	0.005 (.040)	-0.031 (.022)
C11	-0.079 (.036)	0.311 (.024)
C12	0.029 (.042)	0.035 (.024)
C13	-0.051 (.042)	-0.114 (.023)
H3	0.080 (.028)	0.152 (.017)
H4	0.091 (.028)	0.190 (.018)
H5	0.048 (.028)	0.130 (.018)
H6	0.055 (.029)	0.091 (.019)
H7	0.031 (.029)	0.104 (.018)
H9	0.056 (.028)	0.117 (.017)
H10	0.097 (.028)	0.161 (.017)
H12	0.054 (.030)	0.108 (.017)
H13	0.031 (.031)	0.115 (.018)
H2N	0.246 (.040)	0.527 (.015)

Table S7. Electrostatic properties of NCLBA.

```
*****************************************************************************
 PAMOC                          Version 2010-07-27                          PAMOC

                    Molecular Electrostatic Multipole Moments
               obtained from different DMA of the electron density
         Units: electrons, Debye, Debye-Ang, Debye-Ang**2, Debye-Ang**3
 Origin: Center of Mass  -  Reference System: Eigen-axes of the inertial tensor
   <NCLBA2>   NCL cpl=0.010; 10.07.21 da lp.tempo3 2a + 3a racc sec cry; 2021

 M.Barzaghi@istm.cnr.it                                   www.istm.cnr.it/pamoc
 *****************************************************************************

-------------------------------------------------------------------------
 Traceless Cartesian Tensors
 -------------------------------------------------------------------------
             L         <O>     Stewart (   esds   )       QTAIM (   esds   )
 -------------------------------------------------------------------------

          1  0  0      <q>      0.0000 (    0.0000)      0.0000 (    0.0000)

          2  1  1      <x>      3.3051 (    1.1121)      3.6247 (    1.0011)
          3  1  2      <y>     -3.1749 (    1.2983)     -3.0622 (    0.9385)
          4  1  3      <z>     -0.1303 (    1.0275)     -0.0985 (    0.5238)

                     Dipole      4.5848 (    0.9605)      4.7461 (    0.6003)

          5  2  1     <xx>    -26.7291 (    5.0784)    -25.1837 (    6.8059)
          6  2  2     <xy>     22.1901 (    3.9881)     21.8188 (    4.3187)
          7  2  3     <yy>     13.4098 (    4.7394)     12.3772 (    5.9101)
          8  2  4     <xz>     -4.0570 (    2.1038)     -3.9900 (    2.4549)
          9  2  5     <yz>     -1.9954 (    2.2769)     -2.1960 (    2.4693)
         10  2  6     <zz>     13.3193 (    2.3758)     12.8064 (    2.6895)

    (<xx> + <yy> + <zz>)/3      0.0000 (    0.0000)      0.0000 (    0.0000)
                Anisotropy      7.4893 (    0.5395)      7.3494 (    0.7033)

         11  3  1    <xxx>     13.5044 (   16.4410)     18.4361 (   32.7476)
         12  3  2    <yyy>     83.4199 (   14.0962)     84.2000 (   22.9535)
         13  3  3    <zzz>    -11.1537 (   13.5617)    -12.7298 (   17.0545)
         14  3  4    <xyy>     32.8420 (   12.8879)     31.7252 (   22.7341)
         15  3  5    <xxy>    -67.8919 (   12.1178)    -68.1637 (   21.0037)
         16  3  6    <xxz>     56.7001 (   10.0689)     57.0726 (   13.4823)
         17  3  7    <xzz>    -46.3463 (   11.5389)    -50.1613 (   23.2010)
         18  3  8    <yzz>    -15.5280 (   11.7689)    -16.0363 (   16.6862)
         19  3  9    <yyz>    -45.5464 (    9.1931)    -44.3428 (   13.8590)
         20  3 10    <xyz>    -24.8764 (    7.5278)    -24.3045 (   10.7909)

     <xxx> + <xyy> + <xzz>      0.0000 (    0.0000)      0.0000 (    0.0000)
     <yyy> + <xxy> + <yzz>      0.0000 (    0.0000)      0.0000 (    0.0000)
     <zzz> + <xxz> + <yyz>      0.0000 (    0.0000)      0.0000 (    0.0000)
  Magnitude of vector part      0.0000 (    0.0000)      0.0000 (    0.0000)
   Project. on dipole dir.      0.0000 (    0.0000)      0.0000 (    0.0000)

         21  4  1   <xxxx>   -135.8839 (   86.7214)    -97.3262 (  333.8155)
         22  4  2   <yyyy>    -97.3003 (   69.0714)    -81.6378 (  164.7968)
         23  4  3   <zzzz>   -401.3795 (   54.4895)   -393.2643 (  140.7862)
         24  4  4   <xxxy>   -222.0777 (   67.7004)   -212.3872 (  170.4764)
         25  4  5   <xxxz>    -34.1662 (   40.7199)    -26.6456 (   98.0714)
         26  4  6   <yyyx>    223.6825 (   78.6435)    212.9915 (  196.6390)
```

```
        27  4  7   <yyyz>    197.3588 (   42.7574)    191.8123 (   94.9110)
        28  4  8   <zzzx>     93.1131 (   33.9757)     91.4009 (   95.4273)
        29  4  9   <zzzy>    120.1422 (   42.1989)    125.6857 (   96.4758)
        30  4 10   <xxyy>    -84.0976 (   61.7704)   -107.1501 (  186.3519)
        31  4 11   <xxzz>    219.9815 (   47.9901)    204.4764 (  172.7155)
        32  4 12   <yyzz>    181.3980 (   48.6390)    188.7880 (  120.5702)
        33  4 13   <xxyz>   -317.5010 (   30.0437)   -317.4980 (   70.4613)
        34  4 14   <yyxz>    -58.9469 (   40.6247)    -64.7553 (   80.4396)
        35  4 15   <zzxy>     -1.6049 (   32.1860)     -0.6043 (   68.7406)

 <xxxx> + <xxyy> + <xxzz>      0.0000 (    0.0000)      0.0000 (    0.0000)
 <yyyy> + <xxyy> + <yyzz>      0.0000 (    0.0000)      0.0000 (    0.0000)
 <zzzz> + <yyzz> + <xxzz>      0.0000 (    0.0000)      0.0000 (    0.0000)
 <xxxy> + <yyyx> + <zzxy>      0.0000 (    0.0000)      0.0000 (    0.0000)
 <xxxz> + <zzzx> + <yyxz>      0.0000 (    0.0000)      0.0000 (    0.0000)
 <yyyz> + <zzzy> + <xxyz>      0.0000 (    0.0000)      0.0000 (    0.0000)
          Isotropic value      0.0000 (    0.0000)      0.0000 (    0.0000)

-------------------------------------------------------------------------------
```

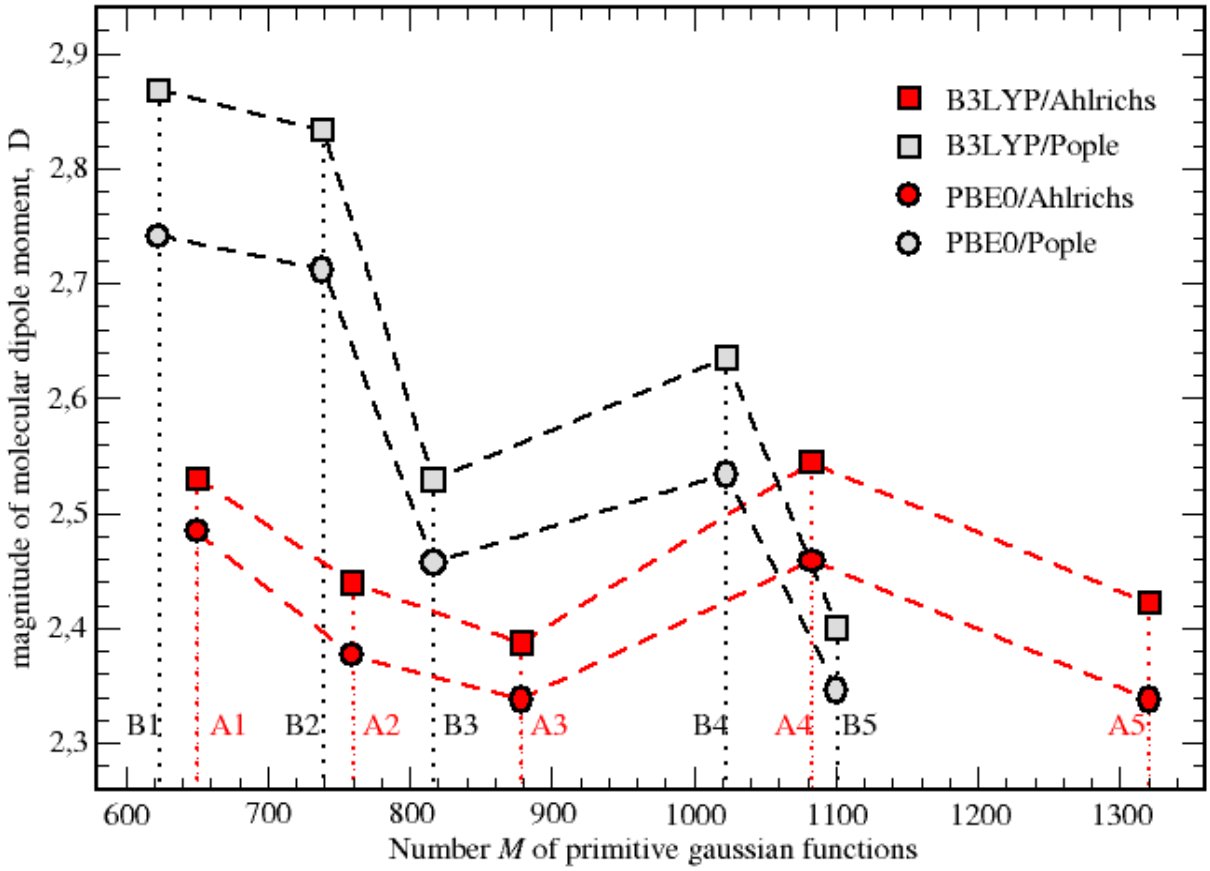

Figure S7: Basis set convergence of the molecular dipole moment magnitude of NCLBA in vacuum for two basis set families (Ahlrichs: red symbols, Pople: grey symbols) and two density functionals (B3LYP: squares, PBE0: circles). For each density functional, the dashed lines connect the points belonging to the same basis set family. Vertical dotted lines mark the individual basis sets (A1: pob-TZVP-rev2, M = 651; A2: def2-TZVP (-f), M = 760; A3: def2-TZVP, M = 879; A4: def2-aug-TZVPP(-f), M = 1083; A5: def2-aug-TZVPP, M = 1321).

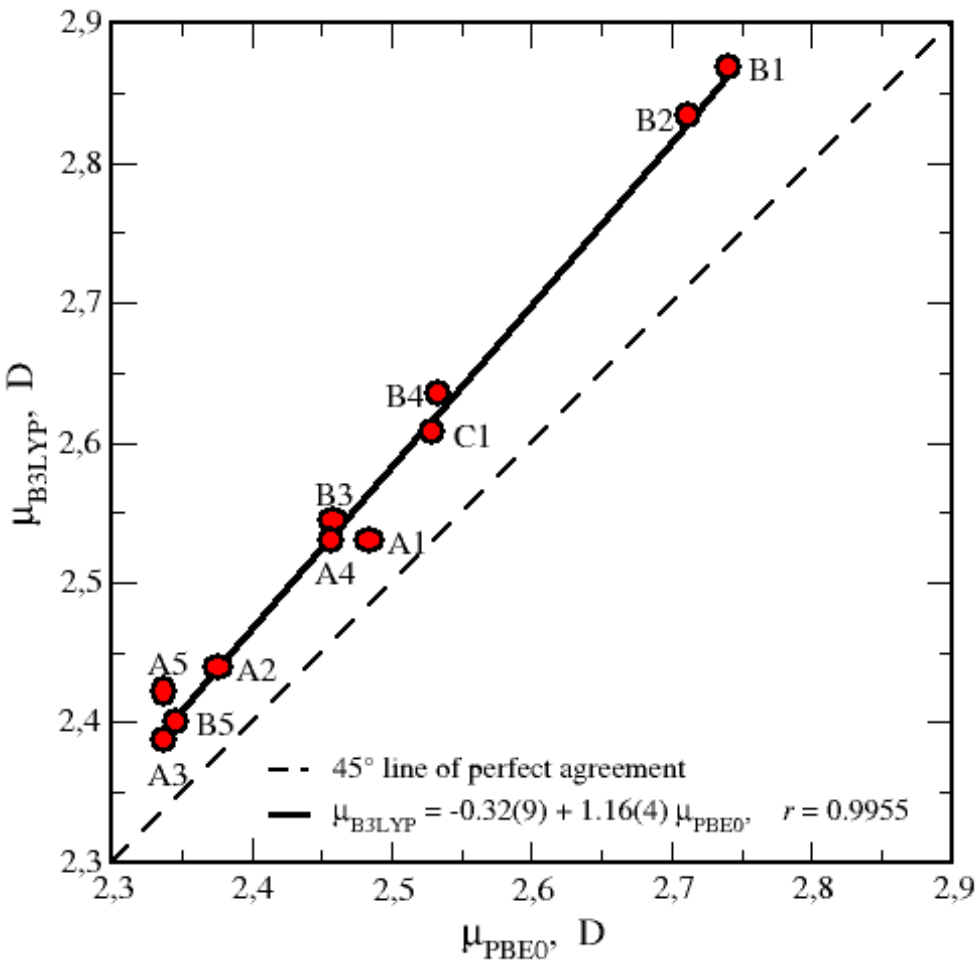

Figure S8. Relationship between B3LYP and PBE0 values of the NCLBA dipole moment magnitude calculated using the basis sets specified in Section S7 above.

Comments to Figures S7 and S8:
Figure S8 shows that the B3LYP predictions somewhat overestimate the magnitude of the molecular dipole. However, two effects that are worth of note. First, the predictions tend to cluster around similar values as the magnitude of the basis set increases. Second, differences between B3LYP and PBE0 hamiltonians become smaller and smaller as the magnitude of the basis set increases. The same information can be retrieved from Figure S7. In our opinion, this is a good indication of convergence. We do not demand that convergence be exact, a requirement that would be fulfilled only in the limit of a complete basis set. The accurate estimation of static electrostatic properties is much more demanding that convergence on geometrical parameters and we consider that our simulations provide a reasonable and satisfactory tradeoff between the required accuracy and the computational cost. In any case, it is worth noting that the experimentally estimated standard deviations on the magnitude of the dipole moment are one order of magnitude larger than differences among the theoretically predicted dipole moment lengths.

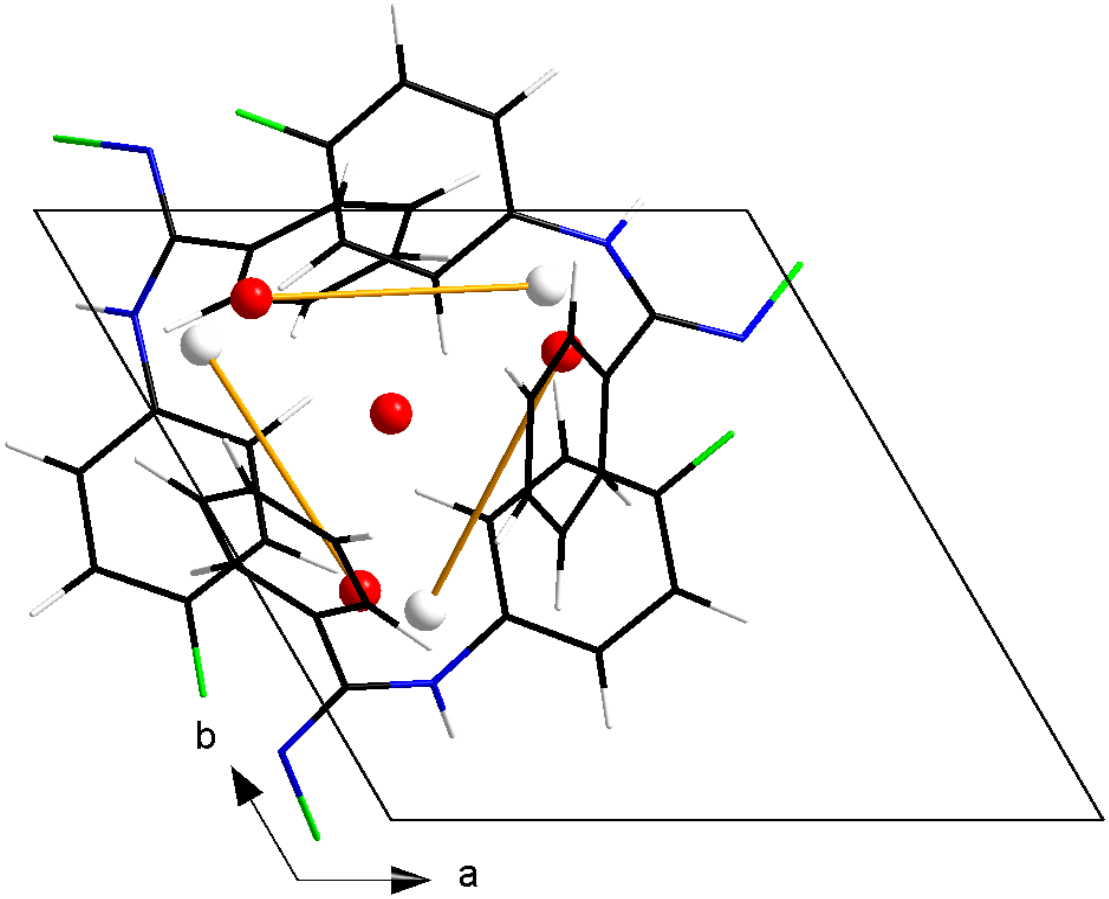

Figure S9. Mutual orientation of molecular dipole moments in the experimental unit cell of NCLBA at T = 17.5 K. White spheres: origin of the dipole moment (molecular centre of mass, negative extremity). Red spheres: positive extremities. The dipole total moment is at the centre of the 3_1 helix motif and points upwards parallel to the *c* axis.

References

(1) Destro, R. Experimental Determination of Scan-Truncation Losses from Low-Temperature (16 K) Single-Crystal X-Ray Measurements. *Aust. J. Phys.* **1988**, *41* (3), 503–510.

(2) Destro, R.; Marsh, R. E. Scan-Truncation Corrections in Single-Crystal Diffractometry: An Empirical Method. *Acta Crystallogr. Sect. A Found. Crystallogr.* **1987**, *43* (5), 711–718.

(3) Destro, R.; Marsh, R. E. On Predicting Scan Profiles: The Nature of the `aberration Function'. *Acta Crystallogr. Sect. A Found. Crystallogr.* **1993**, *49* (1), 183–190.

(4) Destro, R.; Ruffo, R.; Roversi, P.; Soave, R.; Loconte, L.; Lo Presti, L. Anharmonic Motions versus Dynamic Disorder at the Mg Ion from the Charge Densities in Pyrope (Mg3Al2Si3O12) Crystals at 30 K: Six of One, Half a Dozen of the Other. *Acta Crystallogr. Sect. B Struct. Sci. Cryst. Eng. Mater.* **2017**, *73* (4), 722–736.

(5) Gatti, C.; May, E.; Destro, R.; Cargnoni, F. Fundamental Properties and Nature of CH··O Interactions in Crystals on the Basis of Experimental and Theoretical Charge Densities. The Case of 3,4-Bis(Dimethylamino)-3-Cyclobutene-1,2-Dione (DMACB) Crystal. *J. Phys. Chem. A* **2002**, *106* (11), 2707–2720.

(6) Destro, R.; Roversi, P.; Barzaghi, M.; Lo Presti, L. Anharmonic Thermal Motion Modelling in the Experimental XRD Charge Density Determination of 1-Methyluracil at T = 23 K. *Molecules* **2021**, *26* (11), 3075.

(7) Vilela Oliveira, D.; Laun, J.; Peintinger, M. F.; Bredow, T. BSSE-Correction Scheme for Consistent Gaussian Basis Sets of Double- and Triple-Zeta Valence with Polarization Quality for Solid-State Calculations. *J. Comput. Chem.* **2019**, *40* (27), 2364–2376.

(8) Peintinger, M. F.; Oliveira, D. V.; Bredow, T. Consistent Gaussian Basis Sets of Triple-Zeta Valence with Polarization Quality for Solid-State Calculations. *J. Comput. Chem.* **2013**, *34* (6), 451–459.

(9) Adamo, C.; Barone, V. Toward Reliable Density Functional Methods without Adjustable Parameters: The PBE0 Model. *J. Chem. Phys.* **1999**, *110* (13), 6158.

(10) Dovesi, R.; Erba, A.; Orlando, R.; Zicovich-Wilson, C. M.; Civalleri, B.; Maschio, L.; Rérat, M.; Casassa, S.; Baima, J.; Salustro, S.; et al. Quantum-Mechanical Condensed Matter Simulations with CRYSTAL. *Wiley Interdiscip. Rev. Comput. Mol. Sci.* **2018**, *8* (4), 1360.

(11) Weigend, F.; Ahlrichs, R. Balanced Basis Sets of Split Valence, Triple Zeta Valence and Quadruple Zeta Valence Quality for H to Rn: Design and Assessment of Accuracy. *Phys. Chem. Chem. Phys.* **2005**, *7* (18), 3297–3305.

(12) Krishnan, R.; Binkley, J. S.; Seeger, R.; Pople, J. A. Self-consistent Molecular Orbital Methods. XX. A Basis Set for Correlated Wave Functions. *J. Chem. Phys.* **2008**, *72* (1), 650.

(13) Jensen, F. Contracted Basis Sets for Density Functional Calculations: Segmented versus General Contraction. *J. Chem. Phys.* **2005**, *122* (7), 074111.

(14) Stephens, P. J.; Devlin, F. J.; Chabalowski, C. F.; Frisch, M. J. Ab Initio Calculation of Vibrational Absorption and Circular Dichroism Spectra Using Density Functional Force Fields. *J. Phys. Chem.* **2002**, *98* (45), 11623–11627.

(15) Lee, C.; Yang, W.; Parr, R. G. Development of the Colle-Salvetti Correlation-Energy Formula into a Functional of the Electron Density. *Phys. Rev. B* **1988**, *37* (2), 785.

(16) Becke, A. D. Density-functional Thermochemistry. III. The Role of Exact Exchange. *J. Chem. Phys.* **1998**, *98* (7), 5648.

(17) Vosko, S. H.; Wilk, L.; Nusair, M. Accurate Spin-Dependent Electron Liquid Correlation Energies for Local Spin Density Calculations: A Critical Analysis. *Can. J. Phys.* **1980**, *58* (8), 1200–1211.

(18) Grimme, S. Semiempirical Hybrid Density Functional with Perturbative Second-Order Correlation. *J. Chem. Phys.* **2006**, *124* (3), 034108.

(19) Hickey, A. L.; Rowley, C. N. Benchmarking Quantum Chemical Methods for the Calculation of Molecular Dipole Moments and Polarizabilities. *J. Phys. Chem. A* **2014**, *118* (20), 3678–

3687.
(20) Hait, D.; Head-Gordon, M. How Accurate Is Density Functional Theory at Predicting Dipole Moments? An Assessment Using a New Database of 200 Benchmark Values. *J. Chem. Theory Comput.* **2018**, *14* (4), 1969–1981.
(21) Zapata, J. C.; McKemmish, L. K. Computation of Dipole Moments: A Recommendation on the Choice of the Basis Set and the Level of Theory. *J. Phys. Chem. A* **2020**, *124* (37), 7538–7548.